Molecular Dynamics Simulation of Sorption of Gases in Polystyrene

Hossein Eslami*,†,‡ and Florian Müller-Plathe†

Eduard-Zintl-Institut für Anorganische und Physikalische Chemie, Technische Universität Darmstadt, Petersenstrasse 20, D-64287, Germany, and Department of Chemistry, College of Sciences, Persian Gulf University, Boushehr 75168, Iran

Received March 22, 2007; Revised Manuscript Received June 20, 2007

ABSTRACT: A computational method for the calculation of the solubility of gases, including argon, hydrogen, nitrogen, carbon dioxide, methane, and propane, in polystyrene over a wide range of temperatures and pressures is described. The excess chemical potentials and the partial molar volumes of gases in polystyrene were calculated using Widom's test-particle insertion method. Using the calculated chemical potentials and partial molar volumes of the sorbed gases at a fixed temperature, the chemical potentials in the polymer phase were expanded in terms of the pressure. Performing a grand-canonical ensemble molecular dynamics simulation of the gas phase, we calculated the phase coexistence point using a recent method by Vrabec and Hasse [*Mol. Phys.* **2002**, *100*, 3375−3383]. The results on the calculated solubility coefficients and solubilities over a wide range of temperatures and pressures are compared with experimental data.

Introduction

Knowledge of the solubilities of small molecules in polymers is essential for the design and operation of polymer plants so that residual monomers, oligomers, and polymerization solvents can be removed from the polymer products. Gas solubilities also play important roles in such applications as designing polymer barrier materials for packaging applications, developing membranes for gas separations, foaming, and plasticization. For gases in polymers, the solubility describes the concentration of the gas inside a polymer at equilibrium with the gas at a partial pressure P and is often described by the dual-mode sorption theory:[1,2]

$$C = k_H P + C_\infty \frac{bP}{1 + bP} \quad (1)$$

where C is the concentration of the gas in polymer, k_H is the Henry's law solubility coefficient, C_∞ is the saturation concentration of the gas, and b is the affinity coefficient. This model assumes that there are two distinct modes by which a glassy polymer can sorb gas molecules: Henry's law and a Langmuir mechanism which corresponds to the sorption of gases into specific sorption sites in the polymer. The Henry's law constant has the same physical meaning for glassy polymers as it does for rubbery polymers and liquids, whereas the Langmuir-type term is believed to account for gas sorption into interstitial spaces and microvoids, which are consequences of local heterogeneities and are intimately related to the slow relaxation processes associated with the glassy state of the polymer. Local equilibrium is assumed between the two modes.

The dual-mode sorption equation, eq 1, provides a linear relationship against the pressure in the low-pressure region, i.e.

$$C = (k_H + C_\infty b)P = S_0 P \quad (2)$$

where S_0 is called the apparent solubility coefficient in the zero-pressure limit in glassy polymers.

* Corresponding author. E-mail: h.eslami@theo.chemie.tu-darmstadt.de.
† Technische Universität Darmstadt.
‡ Persian Gulf University.

Traditional approaches for the calculation of the phase equilibria and sorption of penetrant molecules in polymers are based on equation-of-state models,[3−5] which take into account the PVT properties of both gas and polymer, and the activity coefficient models,[6,7] which take into account the specific interactions between polymer and penetrant molecules. Molecular simulations are the other attractive method for this type of calculation. These methods do not invoke any approximations, and predictions are based on well-defined molecular characteristics.

Many computational studies of the permeation of small gas molecules through polymers have appeared, which were designed to analyze, on an atomic scale, diffusion mechanisms or to calculate the diffusion coefficient and the solubility parameters. Most of these studies have dealt with flexible polymer chains of relatively simple structure such as polyethylene, polypropylene, and poly(isobutylene).[8−12] There are however a few reports on polymers consisting of stiff chains. For example, Mooney and MacElroy[13] studied the diffusion of small molecules in semicrystalline aromatic polymers, and Cuthbert et al.[14] have calculated the Henry's law constant for a number of small molecules in polystyrene and studied the effect of box size on the calculated Henry's law constants. Most of these reports are limited to the calculation of solubility coefficients at a single temperature and in the zero-pressure limit. However, there are few reports on the calculation of solubilities at higher pressures, for example, the reports by de Pablo et al.[15] on the calculation of solubilities of alkanes in polyethylene, by Abu-Shargh[12] on the calculation of solubility of propene in polypropylene, and by Lim et al.[16] on the sorption of methane and carbon dioxide in amorphous poly(ether imide). In the former two cases, the authors have used the Gibbs ensemble Monte Carlo method[17,18] to do the calculations, and in the latter case, the authors have used an equation-of-state method to describe the gas phase. It is the purpose of this paper to calculate the solubilities of some molecules in polystyrene over a wide range of temperatures and pressures. Instead of using the Gibbs ensemble Monte Carlo method,[17,18] we use a recent method developed by Vrabec and Hasse[19] called grand equilibrium molecular dynamics method, which is shown to be superior to the Gibbs ensemble Monte Carlo method.

10.1021/ma070697+ CCC: $37.00
Published on Web 07/31/2007

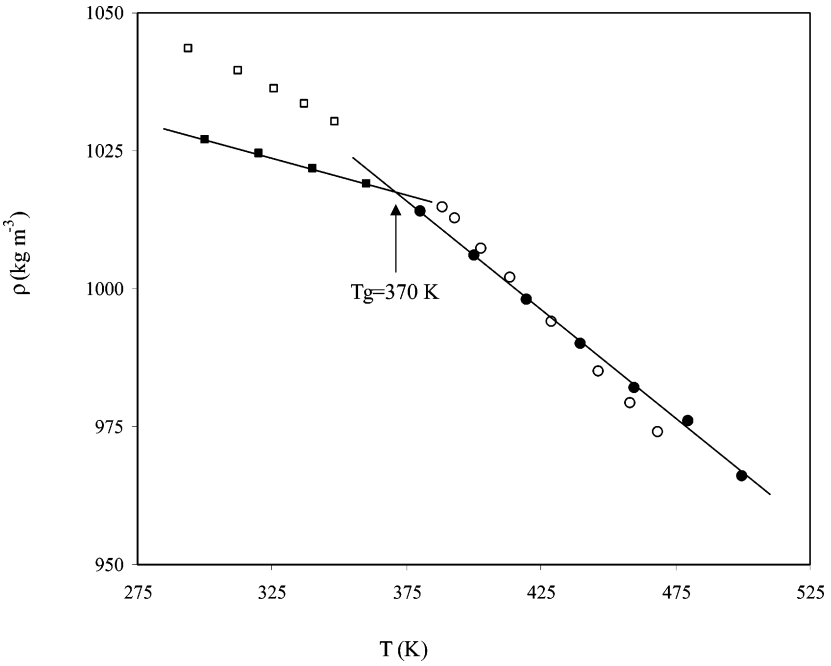

Figure 1. Temperature dependence of the density of polystyrene at 1.0 atm. The filled markers represent our calculations, and the corresponding open markers represent experimental data. The lines represent the best linear fit through the calculated points and the break shows the glass transition temperature.

Table 1. Lennard-Jones Site−Site Potential Parameters for Ar, N_2, and H_2

gas	l (nm)	ϵ (kJ mol^{-1})	σ (nm)	ref
Ar		0.998	0.3405	50
N_2	0.109	0.310	0.331	51
H_2	0.0375	0.093	0.268	52

Table 2. Potential Energy Parameters for Polyatomic Penetrant Gases

		CO_2[53]	
ϵ_C (kJ mol^{-1})	0.239	σ_O (nm)	0.30
ϵ_O (kJ mol^{-1})	0.687	q_C (e)	0.5888
σ_C (nm)	0.2792	l_{C-O} (nm)	0.1163
		CH_4 and C_3H_8[54]	
ϵ_C (kJ mol^{-1})	0.276	θ_{C-C-C} (deg)	112.7
ϵ_H (kJ mol^{-1})	0.1255	k_{C-C-C} (kJ mol^{-1} rad^{-2})	488.5
σ_C (nm)	0.350	k_{H-C-H} (kJ mol^{-1} rad^{-2})	430.0
σ_H (nm)	0.250	θ_{H-C-H} (deg)	110.7
q_H (e)	0.060	θ_{H-C-C} (deg)	107.8
l_{C-C} (nm)	0.1529	$\varphi_{H-C-C-H}$ (deg)	180.0
l_{C-H} (nm)	0.109	$k_{H-C-C-H}$ (kJ mol^{-1})	5.961

Theory

Considering a real gas at temperature T and pressure P in equilibrium with a polymer phase and assuming that at equilibrium the concentration of the sorbed gas inside the polymer is C, we can write the following expression connecting the solubility coefficient to the excess chemical potentials:

$$\mu^{ex}_{\text{gas in polymer}}(T,P) - \mu^{ex}_{\text{gas}}(T,P) = -k_B T \ln(S k_B T) \qquad (3)$$

where k_B is Boltzmann's constant and S is the solubility coefficient defined as C/P. Because of the fact that gas solubilities have been determined by means of different methods, they have been expressed in different units. The most frequently used unit is the volume of gas (in cm^3) reduced to the standard conditions dissolved in 1 cm^3 of polymer, i.e.

$$S = \frac{V_g(\text{STP})}{V_p P} \qquad (4)$$

where V_g(STP) is the volume of the penetrant gas at STP conditions ($T_0 = 273.15$ K and $P_0 = 1$ atm) and V_p is the volume of polymer at temperature T and pressure P. Correspondingly, eq 3 is written as

$$\mu^{ex}_{\text{gas in polymer}}(T,P) - \mu^{ex}_{\text{gas}}(T,P) = -k_B T \ln\left(\frac{\text{STP}_0}{T_0}\right) \qquad (5)$$

At relatively low pressures the second term on the left-hand side of eq 5 is nearly zero and can be neglected.

In this work, the excess chemical potential of a gas sorbed in polystyrene is obtained by applying Widom's test-particle insertion method.[20] In this method a test molecule is inserted randomly into a polymer configuration, and the excess chemical potential is calculated as

$$\mu^{ex} = -k_B T \ln\langle V \exp(-\Delta U/k_B T)\rangle/N \qquad (6)$$

where ΔU is the potential energy of interaction between the test particle and the host polymer, V is the volume, and N is the number of particles. To calculate the excess chemical potential at infinite dilution, first molecular dynamics simulations are performed at a specified temperature and pressure of the polymer, without any gas molecules. After equilibration, several configurations are extracted at different times from the dynamic simulation and used to insert the test particles. A test molecule is repeatedly inserted in random positions and random orientations into the selected configurations, and the energy change due to insertions is calculated. The excess chemical potential is then calculated as the average of the Boltzmann factor of the test particle insertions according to eq 6. This Boltzmann factor is interpreted as the acceptance probability in hypothetical Monte Carlo moves, which would insert a particle into a configuration.

In order to calculate the sorption isotherms, we generate several simulation cells containing polymer and gas molecules at the specified concentrations. The mixture is then relaxed, and the excess chemical potential is calculated using the afore-cited

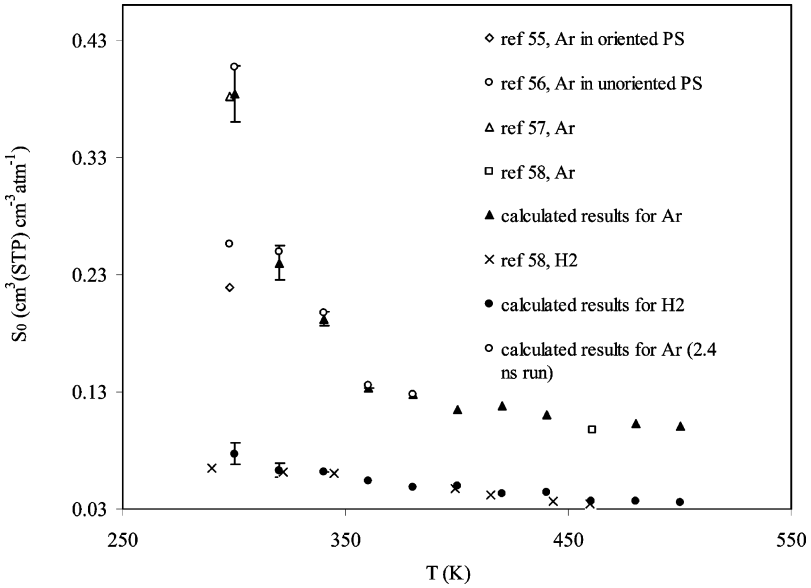

Figure 2. Temperature dependence of the calculated solubility coefficients at zero-pressure limit, S_0, for Ar and H_2 sorbed in polystyrene compared with experimental measurements. For the sake of comparison the calculate results on Ar for a shorter run (a 2.4 ns run) are also indicated in the figure.

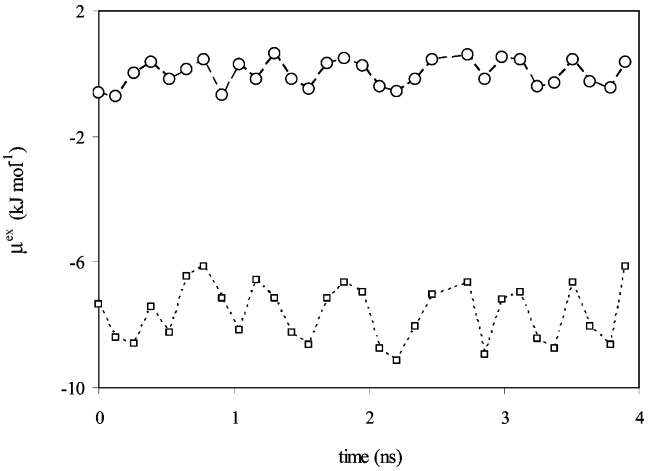

Figure 3. Excess chemical potential at infinite dilution for methane (○) and propane (□) in polystyrene at 300 K and 1.0 atm calculated at 130 ps intervals.

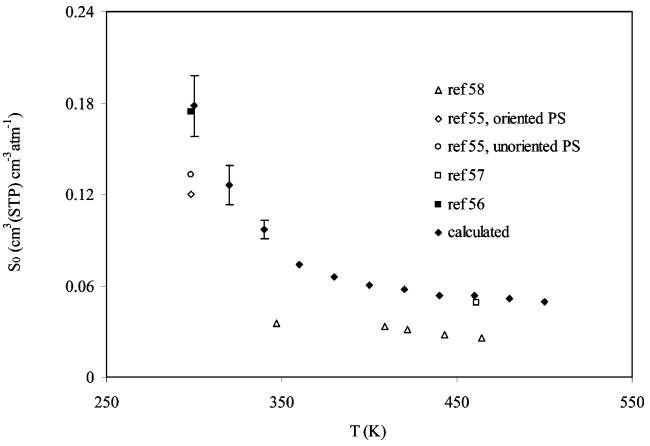

Figure 4. Temperature dependence of S_0 for N_2 sorbed in polystyrene compared with experimental measurements.

procedure. There are several methods for the calculation of phase coexistence points using molecular simulations, such as thermodynamic scaling method,[21,22] histogram reweighting method,[23,24] the Gibbs−Duhem integration method,[25,26] NPT plus test particle method,[27,28] various extensions of it to other ensembles,[29,30] and the Gibbs ensemble Monte Carlo method.[17,18] The last technique has been applied to coexistence properties of simple systems, such as fluids of spherical Lennard-Jones or Yukawa particles,[31,32] as well as more complex systems, such as polyatomic hydrocarbons[33,34] and chain molecules.[35] There are also reports on the mixed methods in which the molecular simulation approaches have been utilized to calculate the chemical potentials in the condensed phase and the results from equations-of-state predictions to calculate the phase coexistence point[16] or to calculate the interaction energy parameters of solvent and polymer, in combination with statistical-mechanical theories for the study of phase equilibria of polymer−solvent mixtures.[36] Here, we apply a new procedure called grand equilibrium molecular dynamics method developed by Vrabec and Hasse[19] to calculate the coexistence point. The method is explained briefly in the following section.

Method

The Gibbs ensemble simulation method specifies the thermodynamic variables temperature, global composition, and global pressure for the simulation of both phases in separate volumes. Practically, this set of thermodynamic variables is in many cases not convenient, and simultaneous simulation of both phases has the disadvantage that fluctuations occurring in one phase influence the other one. Recently a new method, grand equilibrium method, has been developed by Vrabec and Hasse.[19] This method circumvents these problems for the study of phase equilibria. The specified thermodynamic variables are temperature and composition, and two independent simulations are performed for the two phases without the need to exchange particles in the condensed phase. According to this method for a mixture composed of several components, it is possible to do a simulation in the isothermal−isobaric (NPT) ensemble at constant temperature, at constant composition of the condensed phase, and at an arbitrary constant pressure, preferably close to the pressure at the phase coexistence point, to obtain the density of the condensed phase.

In the grand equilibrium method, a simulation of the condensed phase is done to calculate the excess chemical potentials, μ_i^{ex}, and the partial molar volumes, V_i, of all

Table 3. Calculated Excess Chemical Potentials (kJ mol^{-1}) at Infinite Dilution for Gas Molecules in Polystyrene

	T (K)					
gas	300	340	380	420	460	500
Ar	2.65 ± 0.16	5.32 ± 0.18	7.59 ± 0.15	9.00 ± 0.22	10.55 ± 0.17	12.10 ± 0.20
H_2	6.66 ± 0.26	8.52 ± 0.24	10.61 ± 0.22	12.50 ± 0.35	14.73 ± 0.32	16.50 ± 0.27
N_2	4.57 ± 0.33	7.25 ± 0.29	9.67 ± 0.31	11.53 ± 0.41	13.25 ± 0.34	15.05 ± 0.38
CO_2	−3.10 ± 0.44	0.44 ± 0.39	3.79 ± 0.37	6.02 ± 0.52	8.63 ± 0.49	11.77 ± 0.44
CH_4	−0.02 ± 0.30	3.27 ± 0.28	6.23 ± 0.24	8.31 ± 0.31	10.60 ± 0.35	12.82 ± 0.40
C_3H_8	−7.66 ± 0.47	−4.14 ± 0.40	−1.69 ± 0.45	0.10 ± 0.55	2.30 ± 0.59	4.30 ± 0.47

Table 4. Comparison of Our Calculated S_0 Values with Those Reported by Kucukpinar and Doruker[69]

	S_0	
gas	this work	ref 69
Ar	0.384	0.52
N_2	0.178	0.29
CH_4	1.120	1.1
CO_2	3.851	4.6

components. We use the test-particle insertion method to calculate the excess chemical potentials from eq 6. The partial molar volumes can also be calculated using Widom's test particle insertion method[20] as

$$V_i = \frac{\langle V^2 \exp(\Delta U/k_B T)\rangle}{\langle V \exp(\Delta U/k_B T)\rangle} - \langle V\rangle \tag{7}$$

Knowing the parameters V_i and μ_i^{ex} from this simulation, the desired excess chemical potentials as functions of pressure are obtained from a first-order Taylor series expansion, i.e.

$$\mu_i^{ex}(P) = \mu_i^{ex}(P^*) + \frac{V_i}{kT}(P - P^*) \tag{8}$$

where P^* is the target pressure at which the NPT ensemble simulation is done. Once the $\mu_i^{ex}(P)$ is determined from eq 8 by one NPT ensemble simulation of the condensed phase, one vapor/gas simulation has to be performed in the pseudo-grand canonical ensemble (pseudo-μVT). In a common grand canonical ensemble,[37,38] the parameters temperature, volume, and the chemical potential of all species are fixed, while in this pseudo-μVT ensemble simulation, the parameters T and V are fixed in the common way, but instead of fixing the chemical potentials, they are set as a function of the instantaneous pressure in the gas phase. This procedure ensures that equilibrium between the condensed phase and the gas phase is imposed. In a common μVT ensemble simulation, the chemical potentials are set through insertion and deletion of particles by the comparison between the resulting potential energy change and the desired fixed chemical potential. Here, starting from a low density state point, the gas-phase simulation is forced to change its state to the corresponding phase equilibrium state point.

Vrabec and Hasse[19] pointed out that the pseudo-μVT ensemble simulation moves rapidly into the vicinity of the phase equilibrium state point during the equilibration loop. We have employed this method in the present work to compute the sorption isotherms of argon, hydrogen, nitrogen, carbon dioxide, methane, and propane sorbed in polystyrene.

Results and Discussion

Simulations were performed for pure polystyrene and mixtures of polystyrene plus the penetrant gases argon, hydrogen, nitrogen, carbon dioxide, methane, and propane. The potential energy parameters for polystyrene were reported previously by this group.[39] Parameters for aliphatic carbon and hydrogen are those used before for polyolefins,[40] and the phenyl groups of polystyrene were described by the same parameters as the benzene model of Jorgensen and Severance.[41] The parameters for unlike interactions were determined using Lorentz−Bertholet mixing rules.[37] An atactic random polystyrene chain of 200 monomers was generated[39] in vacuum using the rotational isometric state theory with the weights of Rapold.[42] It consists of 46% mesodiads. Molecular dynamics simulations at constant temperature and constant pressure were performed by weak coupling[43] to a temperature bath of 500 K and a pressure bath of 1.0 atm. The coupling times were 0.2 ps for coupling to the thermostat and 2.0 ps for coupling to the barostat, and the time step was 2 fs. All bond lengths were constrained using the SHAKE algorithm.[44,45] For nonbonded interactions, a cutoff distance of 1.1 nm was used, with a reaction field correction for the Coulombic interactions.[46] The effective dielectric constant was taken to be 2.5, which corresponds to the value for amorphous polystyrene. An atomic Verlet neighbor list was used, which was updated every 15 time steps, and the neighbors were included if they were closer that 1.2 nm. In Figure 1, we show the temperature dependence of the computed densities of polystyrene at a pressure of 1.0 atm, computed from molecular dynamics simulations in the NPT ensemble and a stepwise cooling procedure, as well as the experimental[47] densities. All equilibrium configurations at lower temperatures were produced by cooling the system down with a temperature step of 20 K for around 3 ns. The maximum deviation between our calculated densities compared with experiment[47] is 1.4% (at 300 K). As is shown in Figure 1, the density decreases almost linearly at both high and low temperatures with increasing temperature. At atmospheric pressure, a clear change in the slope of the density with respect to temperature occurs at $T_g = 370$ K, and this is an indication of the glass transition. The experimentally determined[47] glass transition temperature at $P = 1$ atm for a sample of polystyrene with a molecular weight of 2.8×10^5 g mol^{-1} is 367 K. The agreement of the calculated glass transition is quite satisfactory despite the obvious difference in the cooling rates: a few K/s in the experiment as compared to 7 K/ns in our MD simulations.

After equilibrating the polystyrene sample at an specified temperature and pressure, we performed a 2.4 ns run and extracted 30 configurations at 80 ps time intervals and did many trial insertions of the test molecules into each configuration. We then calculated the energy change due to the interaction of the test molecule with the host particles and averaged the Boltzmann factor, eq 6, in order to compute the chemical potential of gas molecules sorbed in polystyrene at infinite dilution. Since a finite number of insertions only samples parts of the available conformation space of the test particle, care must be taken that important contributions to the free energy are not missed by poor sampling. We found that inserting 10 000 test particles per configuration is sufficient to stabilize the computed excess chemical potential. The insertion positions and also the molecular orientations are chosen as random. A well-tested random number generator is used for this purpose.[48] In

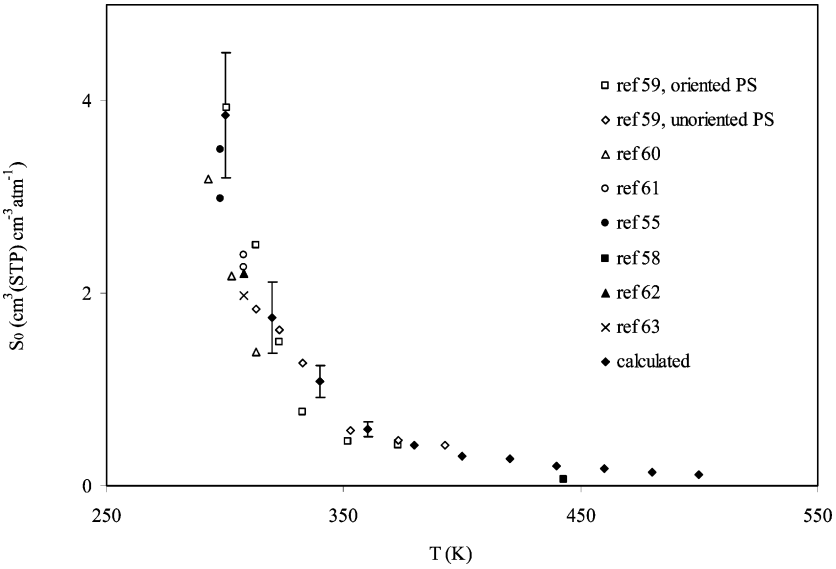

Figure 5. The same as Figure 4 for CO_2.

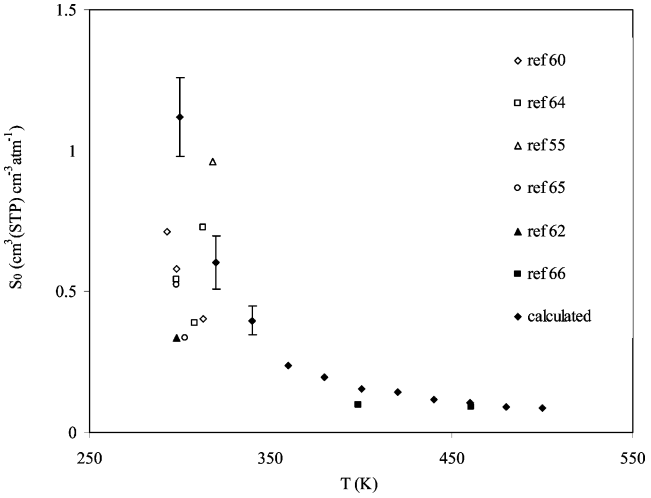

Figure 6. The same as Figure 4 for CH_4.

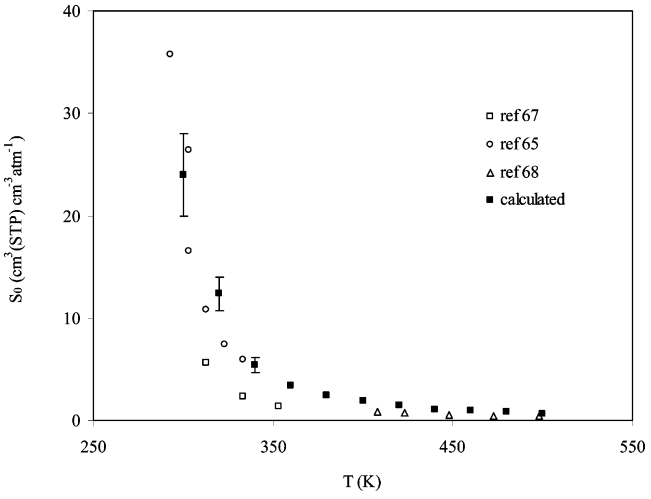

Figure 7. The same as Figure 4 for C_3H_8.

the case of liquids, where the motion of the host molecules provides for sufficient randomness of the local environment at the insertion point, inserting a fixed lattice of test particles also may be used.[49] In the case of polymers with relaxation times much larger than liquids it is believed that random insertions are safer.[8]

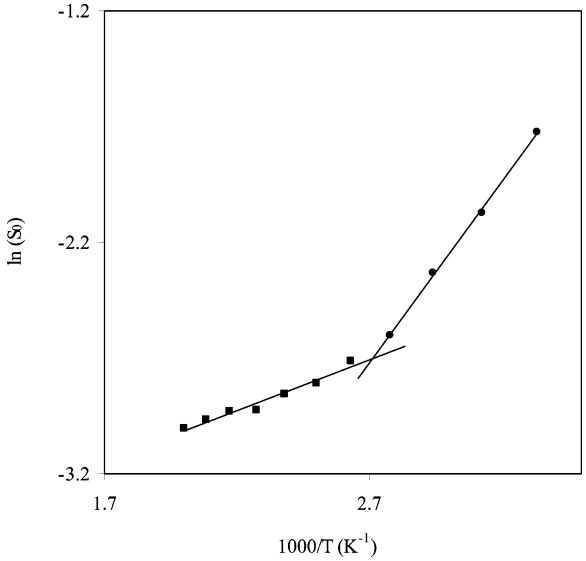

Figure 8. Arrhenius plot of ln(S_0) vs 1/T for N_2 sorbed in polystyrene. The markers show the calculated values, and the lines show the best linear fit through the calculated points.

The Lennard-Jones potential parameters[50−54] used to calculate the interaction energy between gas molecules and polystyrene are reported in Tables 1 and 2. The Lennard-Jones interactions between test molecules and the host polymer are defined by the standard Lorentz−Berthelot mixing rules. The potential is truncated at 1.1 nm, and a standard tail correction is made for the long-range interactions.[37]

Calculating the excess chemical potentials over a 2.4 ns run for Ar as test, we have calculated its solubility coefficients in the zero-pressure limit, S_0, according to eq 5. The results are indicated in Figure 2 and are compared with experimental measurements[55−67] compiled by Paterson et al.[68] As it is seen in Figure 2, our calculated values of S_0 are higher than the corresponding experimental values. Similar differences between experimentally and computed solubility coefficients values have been observed in previous studies.[16,69] As was found earlier by Knopp and Suter,[70] there is an error of $(2-4)k_BT$ commonly found in the calculation of Helmholtz energies by molecular simulations. Moreover, the main contribution to the solubility comes from single holes in the simulated polymer structure, which might not be present in similar proportion in real

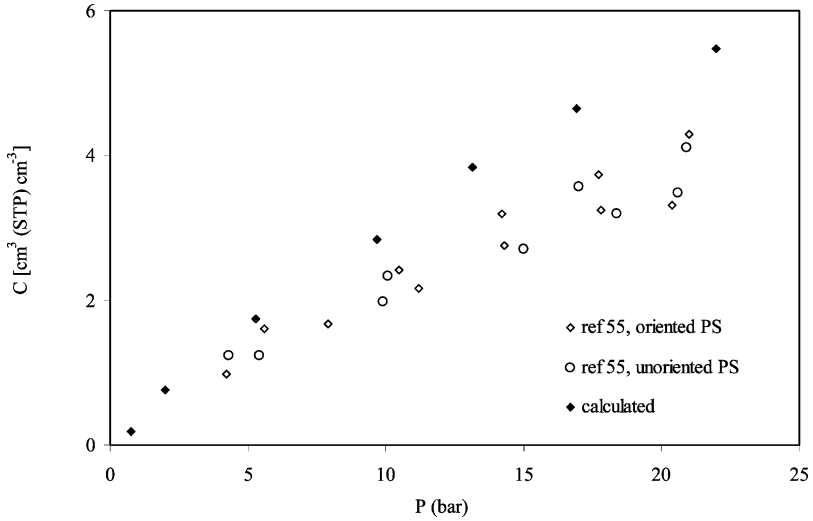

Figure 9. Sorption isotherms for Ar in polystyrene at 298 K.

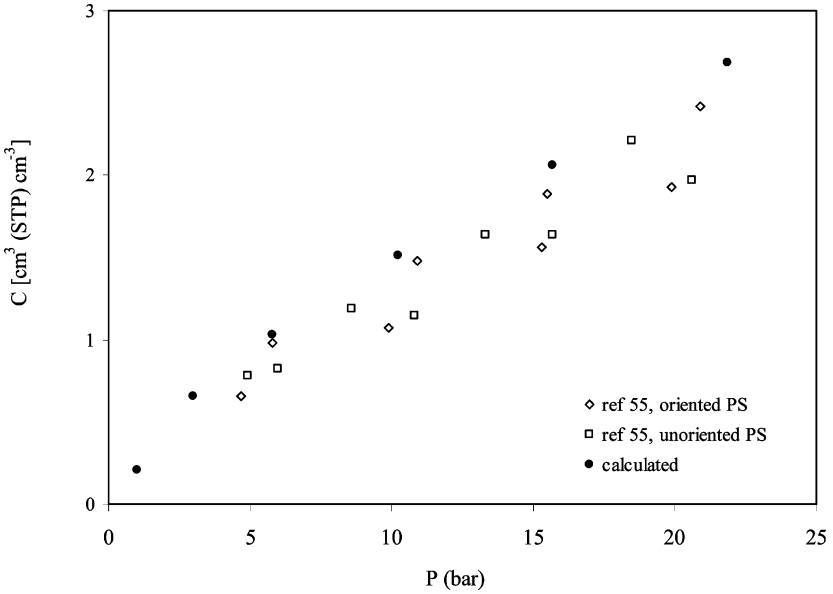

Figure 10. The same as Figure 9 for N_2.

polymers.[71] In order to check whether the configurations generated at 80 ps intervals over a span of 2.4 ns is sufficient to have a good sampling especially in the glassy state, we have performed a longer run, 3.9 ns, and extracted 30 configurations at 130 ps intervals to calculate the excess chemical potentials and hence the solubility coefficients. The calculated results on the solubility coefficient of Ar sorbed in polystyrene for this longer run are also shown in Figure 2. Our results show that the two runs shows a maximum deviation of around 5% at 300 K, while the deviations reduce by a factor of 10 at 380 K. The results shown in Figure 2 show that the calculated S_0 values from the longer run stay lower (get closer to experiment). Considering the overall deviation trend of the calculated S_0 values compared with experiment, we can conclude that the configurations generated at 130 ps time intervals over a time span of 3.9 ns are independent enough for sub-T_g regions; therefore, we decided to do all the calculations for a period of 3.9 ns at $T \leq 380$ K and for a period of 2.4 ns at $T > 380$ K.

The calculated excess chemical potentials from 300 to 500 K in 40 K intervals for Ar, H_2, N_2, CO_2, CH_4, and C_3H_8 are tabulated in Table 3. For methane, and more importantly for propane, we first sampled their conformations in the gas phase and did Widom insertions in an ensemble of internal conformations.

The variations of the infinite-dilution excess chemical potentials with time for CH_4 and C_3H_8 at 300 K over the whole 3.9 ns of simulation are shown in Figure 3. The fluctuations for C_3H_8 are larger than that of CH_4. This is reasonable because of the larger size of C_3H_8 compared to CH_4. In fact, a trial insertion will be done "successfully" if the particle enters a cavity, which is bigger than the particle. The number of smaller cavities in a configuration is much larger than the number of bigger ones; therefore, the number of small cavities is more likely to remain essentially unchanged between two polymer configurations than the number of bigger ones. If the cavity size is big enough, such cavities may altogether disappear and reappear between two configurations. In a glassy polymer it takes a relatively long time of disappearance and reappearance of big cavities. In this case calculation of free energies for bigger molecules is less reliable.

The calculated solubility coefficients in the zero-pressure limit, S_0, according to eq 5, for Ar, H_2, N_2, CO_2, CH_4, and C_3H_8 are shown in Figures 2 and 4−7 and are compared with experimental measurements[55−67] compiled by Paterson et al.[68]

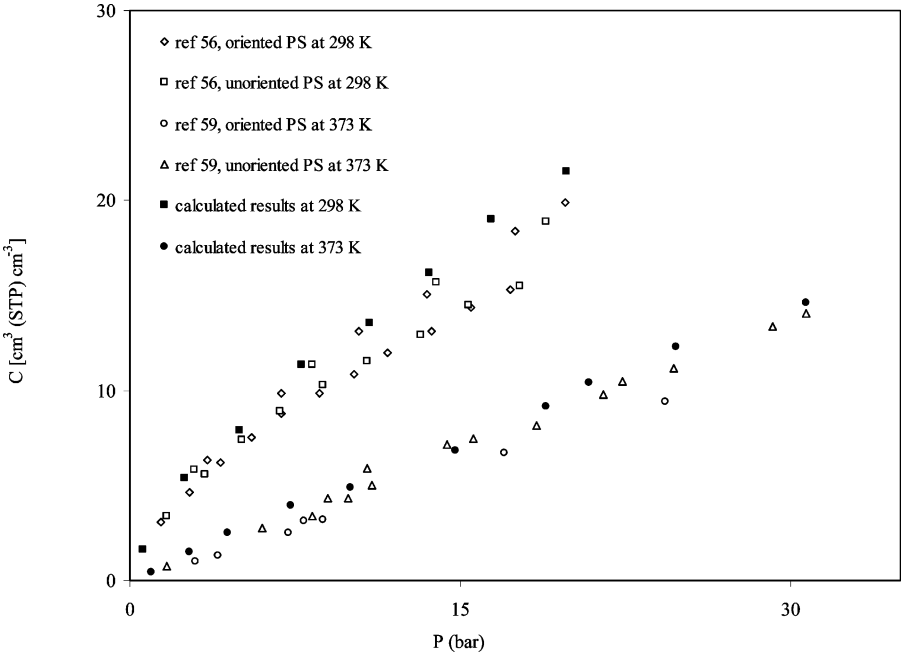

Figure 11. The same as Figure 9 for CO_2.

Since there is no reported experimental measurement of the solubility of C_2H_6 in polystyrene, we did not do calculations for this system. Our calculated values of S_0 are higher than the corresponding experimental values by a factor of 1.25−1.75. We have also compared our calculated S_0 values at 300 K with those of Kucukpinar and Doruker,[69] calculated using free volume calculations done by the transition state approach of Gusev et al.,[72] in Table 4. Although our calculated S_0 values are higher than the corresponding experimental values, the results in Table 4 show that our calculations are still in better agreement with experiment compare to the calculated values of Kucukpinar and Doruker.[69]

To examine the temperature dependence of the calculated solubility coefficients, shown in Figure 8 is the Arrhenius plot of $\ln(S_0)$ with respect to the reciprocal temperature for N_2 as a typical example. As is shown in Figure 8, there are two different slopes to the curve, corresponding to two mechanisms for solubility: Langmuir's mechanism at lower temperatures and Henry's law mechanism at higher temperatures with respect to the glass transition temperature. The calculated value for the enthalpy of sorption below glass transition temperature, as is calculated from the slope of the plot in Figure 8, is −13.0 kJ mol^{-1}, which is comparable to its experimental[56] value at 298 K, −13.8 kJ mol^{-1}. This shows that although the calculated values of solubility coefficients in the zero-pressure limit are higher than the experimentally measured values, their temperature dependencies is calculated more accurately.

We can also compare the calculated solubility ratios with the corresponding values from experimental measurements. We have calculated the ratios of solubility coefficients in the zero-pressure limit to that of Ar and compared the results with experiment in Table 5. Since there is no experimental measurement of the solubility coefficient of H_2 at or close to 300 K, we could not compare our results for H_2 in Table 5. For propane, there is a large inconsistency between experimentally measured solubility coefficients at temperatures close to 300 K. Here we got a ratio of 43.6 from extrapolation of experimental data reported by Yavorsky[67] and a ratio of 101.2 from experimental data reported by Barrie et al.[65] As is clear from Table 5, the calculated ratios are within the experimentally obtained values.

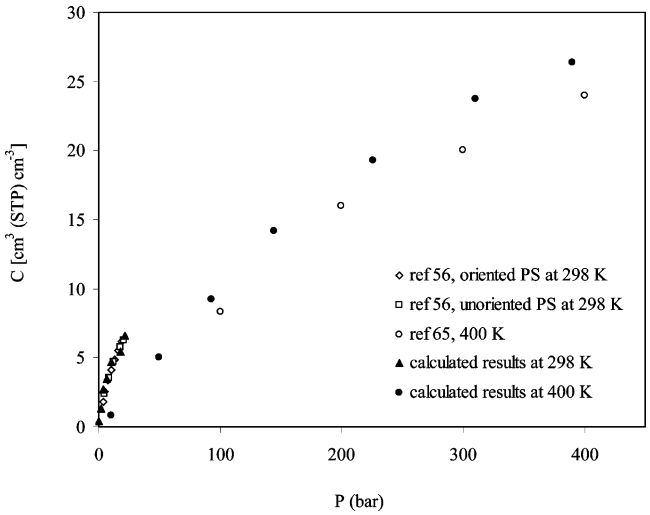

Figure 12. The same as Figure 9 for CH_4.

This confirms that the calculated values of the solubility coefficient are higher with respect to the experimental measurements nearly by the same factor.

To compute the sorption isotherms, we generated many simulation boxes of polystyrene and gas molecules at the specified composition and did molecular dynamics simulation at constant temperature and at a constant pressure, close to the experimental coexistence point. To insert gas molecules into the polymer, we used our implemented grand-canonical ensemble molecular dynamics method[38] and fixed the code so that it always inserts the molecules into the simulation box, until getting the desired number of inserted molecules. In fact, we insert a fractional molecule and grow it to a full molecule with the passage of time. When the fractional molecule grows up to a full molecule, we add it, as an indistinguishable penetrant molecule, to the system and then insert the next fractional molecule and so on. We continue this until reaching the desired concentration of the gas in polystyrene. Having obtained an equilibrated mixture of polystyrene with gas molecules at a fixed temperature and pressure for a period of 3.9 ns, we applied Widom's test particle method[20] to compute the excess chemical

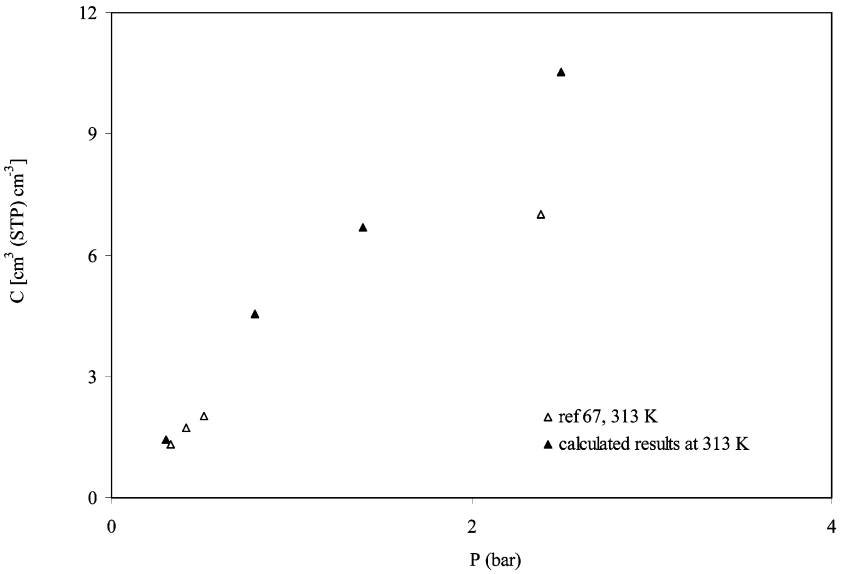

Figure 13. The same as Figure 9 for C_3H_8.

Table 5. Comparison of the Calculated and Experimental Ratios of Solubility Coefficients of Gases with Respect to Ar at 300 K and Zero-Pressure Limit

	$S_0/(S_0)_{Ar}$		
gas	calculated	experimental	ref
N_2	0.46	0.50	55, 56
CO_2	10.0	10.0	60
CH4	2.91	2.85	64
C_3H_8	62.4	43.6−101.2	67, 65

potential and the partial molar volume of the sorbed gas, as described above. Then we performed a pseudo-grand-canonical ensemble molecular dynamics simulation in the gas phase to calculate the coexistence point. Setting the values of chemical potential, temperature, and volume as independent thermodynamic variables, we choose one of the penetrant molecules in the box as a fractional molecule. A fractional molecule is a molecule whose potential energy of interaction to the rest of the system is scaled somehow by a fractional number, ν, ranging between 0 and 1. We compute the variation of the potential energy of the fractional molecule with respect to ν and compare it with the desired value of the excess chemical potential to obtain the acceleration on this new coordinates, ν, and solve the equation of motion. If the fractional molecule grows up, until $\nu = 1$, we incorporate it into the system as a new molecule and insert a new fractional molecule in the simulation box. On the other hand, if ν goes down to zero, we eliminate this molecule from the system and choose one of the molecules in the simulation box as the new fractional molecule and continue the simulation. More details for performing grand-canonical ensemble molecular dynamics simulation are described elsewhere.[38] The computed sorption isotherms for the gases subject to the present work are plotted in Figures 9−13. From the reported results in Figures 9−13 it is clear that our calculated solubilities tend to show higher slopes at low pressures in accordance with our calculations in the zero-pressure limit. Consequently, we predict higher solubility isotherms compared to the experimental solubility isotherms. Considering the inconsistencies between experimental measurements,[55,5,59] as evident in Figures 9−13, our predictions are more or less within the uncertainty range of experimental measurements. For CO_2 at 373 K, our calculated Henry's law constant is in close agreement with experiment[59] (Figure 5). Therefore, also the calculated solubility isotherm in Figure 11 is close to the experiment.[59] For C_3H_6 at 313 K, on the other hand, there is a larger discrepancy between our calculated solubility isotherm and the corresponding experimental isotherm.[67] Part of this disagreement, maybe, is due to the large experimental uncertainty between the reported values of solubility coefficients by the same author[67] compared to the other sources[65,68] (Figure 7).

Conclusions

We have employed a new molecular dynamics simulation method to calculate the solubility coefficients of gases in polystyrene. We need to perform two separate simulations—one simulation in NPT ensemble of the polymer phase and one simulation in pseudo-μVT ensemble of the gas phase—instead of doing simultaneous simulations of both phases which is usually done in the Gibbs ensemble Monte Carlo method. There is no need to exchange particles between two phases. The excess chemical potentials in the polymer phase are calculated using Widom's test-particle insertion method. One advantage of this method is that once we have an equilibrated sample of polystyrene, it can be used for inserting as many gaseous compounds as we need; i.e., there is no need to do another simulation of the polymer phase to calculate the excess chemical potential of another gas. A correct trend is calculated for the solubility coefficients of gases with temperature. Although the calculated solubility coefficients are higher than the experimental ones, as it is often found for solubility coefficients calculated using molecular simulation methods, the ratio of solubility coefficients (selectivity) is quite close to the corresponding experimental data. The overall accuracy of the calculated sorption isotherms depends on the initial slope, S_0, calculated using test-particle method.

Acknowledgment. The support of this work by Alexander von Humboldt Foundation is gratefully acknowledged.

References and Notes

(1) Stannett, V. T.; Koros, W. J.; Paul. D. R.; Lonsdale, H. K.; Baker, R. W. *Adv. Polym. Sci.* **1978**, *32*, 69−121.
(2) Frederickson, G. H.; Helfand, E. *Macromolecules* **1985**, *18*, 2201−2207.
(3) Lacombe, R. H.; Sanchez, I. C. *J. Phys. Chem.* **1976**, *80*, 2568−2580.
(4) Sanchez, I. C.; Rodgers, P. A. *Pure Appl. Chem.* **1990**, *62*, 2107−2114.

(5) von Solms, N.; Michelsen, M. L.; Kontogeorgis, G. M. *Ind. Eng. Chem. Res.* **2005**, *44*, 3330−3335.
(6) Sukhadia, T. Ph.D. Dissertation, Georgia Institute of Technology, Atlanta, GA, 1999.
(7) Ozkan, I. A.; Teja, A. S. *Fluid Phase Equilib.* **2005**, *228*−*229*, 487−491.
(8) Müller-Plathe, F. *Macromolecules* **1991**, *24*, 6475−6479.
(9) Krishna Pant, P. V.; Boyd, R. H. *Macromolecules* **1993**, *26*, 679−686.
(10) Tamai, Y.; Tanaka, H.; Nakanishi, K. *Macromolecules* **1995**, *28*, 2544−254.
(11) Pricl, S.; Fermeglia, M. *Chem. Eng. Commun.* **2003**, *190*, 1267−1292.
(12) Abu-Shargh, B. F. *Polymer* **2004**, *45*, 6383−6389.
(13) Mooney, D. A.; MacElroy, J. M. D. *J. Chem. Phys.* **1999**, *110*, 11087−11093.
(14) Cuthbert, T. R.; Wagner, N. J.; Paulaitis, M. E. *Macromolecules* **1997**, *30*, 3058−3065.
(15) de Pablo, J. J.; Laso, M.; Suter, U. W. *Macromolecules* **1993**, *26*, 6180−6183.
(16) Lim, S. Y.; Tsotsis, T. T.; Sahimi, M. *J. Chem. Phys.* **2003**, *119*, 496−504.
(17) Vrabec, J.; Fischer, J. *Mol. Phys.* **1995**, *85*, 781−792.
(18) Panagiotopoulos, A. Z. *Mol. Phys.* **1987**, *61*, 813−826.
(19) Vrabec, J.; Hasse, H. *Mol. Phys.* **2002**, *100*, 3375−3383.
(20) Widom, B. *J. Chem. Phys.* **1963**, *39*, 2808−2812.
(21) Valleau, J. P. *J. Comput. Phys.* **1991**, *96*, 193−216.
(22) Valleau, J. P.; Graham, I. S. *J. Phys. Chem.* **1990**, *94*, 7894−7898.
(23) McDonald, I. R.; Singer, K. *Discuss. Faraday Soc.* **1967**, *43*, 40−49.
(24) Potoff, J. J.; Panagiotopoulos, A. Z. *J. Chem. Phys.* **1998**, *109*, 10914−10920.
(25) Kofke, D. A. *Mol. Phys.* **1993**, *78*, 1331−1336.
(26) Kofke, D. A. *J. Chem. Phys.* **1993**, *98*, 4149−462.
(27) Boda, D.; Liszi, J.; Szalai, I. *Chem. Phys. Lett.* **1995**, *235*, 140−145.
(28) Boda, D.; Winkelmann, J.; Liszi, J.; Szalai, I. *Mol. Phys.* **1996**, *87*, 601−624.
(29) Boda, D.; Kristof, T.; Liszi, J.; Szalai, I. *Mol. Phys.* **2001**, *99*, 2011−2022.
(30) Moller, D.; Fischer, J. *Mol. Phys.* **1990**, *69*, 463−473.
(31) Panagiotopoulos, A. Z.; Quirke, N.; Stapleton, M.; Tildesley, D. J. *Mol. Phys.* **1988**, *63*, 527−535.
(32) Rudisill, E. N.; Cummings, P. T. *Mol. Phys.* **1989**, *68*, 629−635.
(33) de Pablo, J. J.; Prausnitz, J. M. *Fluid Phase Equilib.* **1989**, *53*, 177−189.
(34) de Pablo, J. J.; Bonnin, M.; Prausnitz, J. M. *Fluid Phase Equilib.* **1992**, *73*, 187−210.
(35) de Pablo, J. J. *Fluid Phase Equilib.* **1995**, *104*, 195−206.
(36) Jang, J. G.; Bae, Y. C. *J. Chem. Phys.* **2002**, *116*, 3484−3492.
(37) Allen, M. P.; Tildesley, D. J. *Computer Simulation of Liquids*; Clarendon Press: Oxford, 1987.
(38) Eslami, H.; Müller-Plathe, F. *J. Comput. Chem.*, in press.
(39) Müller-Plathe, F. *Macromolecules* **1996**, *29*, 4782−4791.
(40) Müller-Plathe, F. *J. Chem. Phys.* **1995**, *103*, 4346.
(41) Jorgensen, W. L.; Severance, D. L. *J. Am. Chem. Soc.* **1990**, *112*, 4768−4774.
(42) Rapold, R. F. Ph.D. Thesis, Swiss Federal Institute of Technology Zürich, 1993.
(43) Berendsen, H. J. C.; Postma, J. P. M.; van Gunsteren, W. F.; DiNola, A.; Haak, J. R. *J. Chem. Phys.* **1984**, *81*, 3684−3690.
(44) Ryckaert, J. P.; Ciccotti, G.; Berendsen, H. J. C. *J. Comput. Phys.* **1997**, *23*, 327−341.
(45) Müller-Plathe, F.; Brown, D. *Comput. Phys. Commun.* **1991**, *64*, 7−14.
(46) Müller-Plathe, F. *Comput. Phys. Commun.* **1993**, *78*, 77−94.
(47) Quach, A.; Simha, R. *J. Appl. Phys.* **1971**, *42*, 4592−4606.
(48) Marsaglia, G.; Zaman, A.; Tsang, W. W. *Stat. Prob. Lett.* **1990**, *8*, 35−39.
(49) Romano, S.; Singer, K. *Mol. Phys.* **1979**, *37*, 1765−1772.
(50) Hansen, J. P.; McDonald, I. R. *Theory of Simple Liquids*; Academic Press: London, 1976.
(51) Cheung, P. S. Y.; Powles, J. G. *Mol. Phys.* **1975**, *30*, 921−938.
(52) Bouanich, J. P. *J. Quant. Spectrosc. Radiat. Transfer* **1992**, *47*, 243−250.
(53) Zhang, Z.; Duan, Z. *J. Chem. Phys.* **2005**, *122*, 214507−2145015.
(54) Chen, B.; Martin, M. G.; Siepmann, J. I. *J. Phys. Chem. B* **1998**, *102*, 2578−2586.
(55) Vieth, W. R.; Tam, P. M.; Michaels, A. S. *J. Colloid Interface Sci.* **1966**, *22*, 360−370.
(56) Odani, H.; Taira, K.; Nemoto, N.; Kurata, M. *Bull. Inst. Chem. Res.* **1979**, *57*, 226.
(57) Durill, P. L.; Griskey, R. G. *AIChE J.* **1965**, *12*, 1147−1151.
(58) Newitt, D. M.; Weale, K. E. *J. Chem. Soc.* **1948**, 1541.
(59) Carfagna, C.; Nicodemo, L.; Nicolais, L.; Campanile, G. *J. Polym. Sci., Part B: Polym. Phys.* **1986**, *24*, 1805.
(60) Sada, E.; Humazawa, H.; Yakushiji, H.; Bamba, Y.; Sakata, K.; Wang, S.-T. *Ind. Eng. Chem. Res.* **1987**, *26*, 433−438.
(61) Puleo, A. C.; Muruganandam, N.; Paul, D. R. *J. Polym. Sci., Part B: Polym. Phys.* **1989**, *27*, 2385.
(62) Raymond, P. C.; Paul, D. R. *J. Polym. Sci., Part B: Polym. Phys.* **1990**, *28*, 2079−2102.
(63) Toi, K.; Paul, D. R. *Macromolecules* **1982**, *15*, 1104−1107.
(64) Vieth, W. R.; Frangoulis, C. S.; Rionda, J. A. *J. Colloid Interface Sci.* **1966**, *22*, 454−461.
(65) Barrie, J. A.; Williams, M. J. L.; Munday, K. *Polym. Eng. Sci.* **1980**, *20*, 21.
(66) Lundberg, J. L.; Mooney, E. J.; Rogers, C. E. *J. Polym. Sci., Part A* **1969**, *7*, 947.
(67) Yavorsky, J. A. Ph.D. Dissertation, Department of Chemistry and Geology, Clemson University, 1984.
(68) Paterson, R.; Yampoi'skii, Y.; Fogg, P. G. T. *J. Phys. Chem. Ref. Data* **1999**, *28*, 1255−1450.
(69) Kucukpinar, E.; Doruker, P. *Polymer* **2003**, *44*, 3607−3620.
(70) Knopp, B.; Suter, U. W. *Macromolecules* **1997**, *30*, 6114−6119.
(71) Müller-Plathe, F.; Rogers, S. C.; van Gunsteren, W. F. *J. Chem. Phys.* **1993**, *98*, 9895−9904.
(72) Gusev, A. A.; Müller-Plathe, F.; van Gunsteren, W. F.; Suter, U. W. *Adv. Polym. Sci.* **1994**, *116*, 207−214.

MA070697+